Some electrochemical features of the *in vivo* corrosion of dental amalgams

M. J. GROSS*, J. A. HARRISON†

*Department of Prosthodontics, Dental School and †School of Chemistry, University of Newcastle-on-Tyne, Newcastle-on-Tyne NE1 7RU, UK

The corrosion potentials of freshly implanted Dispersalloy and Amalcap dental amalgams were measured *in vivo*. Impedance and current measurement methods at controlled potential were used to examine the corrosion of electrodes made from dental amalgams and the binary alloys Hg–Sn and Cu–Sn in a Ringer's solution in the absence of dissolved oxygen. These *in vitro* measurements were used to make some deductions about the nature of the corrosion reactions on the amalgams and to make an estimate of the *in vivo* electrochemical corrosion rates. It is deduced that the amalgams *in vivo* are protected from electrochemical mercury dissolution by the dissolution of the other metals, such as zinc, tin and copper. It is suggested that the mechanisms of mercury loss in dental amalgams are by evaporation, by a coupling with the electrochemical dissolution of zinc, if present, and tin and copper and by mechanical wear mainly through an electrochemical mechanism.

1. Introduction

The loss of metal ions and atoms from dental amalgams is an important problem which has been the subject of some press speculation. It is known that mercury and other components in the amalgams may enter the body [1–3] and cause an allergic reaction in some people [4–6]. There are three mechanisms by which mercury can be released from dental amalgams. These are by mechanical abrasion, dissolution or vaporization of the elemental mercury and by electrochemical corrosion. Because of the difficulty of controlling the physical conditions the relative amounts of mercury generated by these different mechanisms are not known with certainty, although an investigation of the rate of vaporization has been carried out [7–14]. The mercury loss due to this mechanism, *in vivo*, is estimated to be about $20 \, \mu g \, day^{-1}$ [9]. It is also not certain whether mercury atoms or ions are more injurious to the body [15, 16]. In the dental literature, for example [17, 18], this problem does not seem to have been fully explored. The electrochemical mechanism for metal loss, however, is amenable to fairly detailed investigation and the present work is an attempt to assess the electrochemical route for the release of the constituent metals of the amalgams, and to decide if this is likely to be an important route for metal loss.

A complete electrochemical investigation of the behaviour of dental amalgams in the mouth would require extensive measurements of the usual kind which are needed in investigations of metal–electrolyte systems. The methods employed would, most probably, include the measurement of steady state current–potential curves, impedance–potential curves and current–time transients between different potentials.

One of the inherent difficulties of electrochemical measurements is that they reflect the involvement of electrons in the electrode reactions but they do not give an absolute indication of what electrode reactions are involved. However in favourable circumstances, by measuring and comparing the behaviour of related electrode materials the electrode reactions can be identified.

It would also be necessary to carry out a qualitative and quantitative chemical analysis of surface films and of the metal ions entering the solution, in order to confirm the interpretation of the electrochemical measurements. Investigations have been reported in the literature [19–22] of the chemical composition of films formed on copper-rich dental amalgams after up to 10 months of corrosion. Unfortunately the potential of the electrodes under investigation was not recorded in these cases. However Moberg [23] has given potential–time curves and an analysis of the metal in solution.

A complete set of measurements, as just outlined, is difficult to achieve and interpret in laboratory experiments outside the mouth. The difficulty is that there are a number of alloying components in dental amalgams, and measurements would need to be carried out on many compositions of amalgam. It might, also, be necessary to carry out measurements on different aqueous phase solutions to be certain of the interpretation. In the mouth there is only limited possibility of obtaining data. However some simpler experiments are possible *in vivo* and with some assumptions they should correlate with the appropriate experiments carried out *in vitro*. The simplifications which will be used in this paper, are: (1) to limit the measurement in the mouth to the corrosion potential against a reference electrode; (2) to assume that the electrochemical

reactions in the mouth are the same as those observed when an amalgam is placed in two-thirds Ringers solution outside the mouth; (3) to assume that in the two-thirds Ringers solution the only electrochemical reactions are the metal dissolution reactions of the constituents of the dental amalgam, oxygen reduction and the reduction of water to form hydrogen; (4) to assume that in the absence of oxygen the steady state anodic current at the corrosion potential in the presence of oxygen represents the corrosion current of material from the metal amalgam. The ions leaving the bulk phase may be incorporated into a film or freely dissolve.

The previous work has consisted largely of the measurement of steady state current–potential curves, for different dental amalgams, at about the corrosion potential. The impedance and hence the charge transfer resistance has also been measured at the corrosion potential. Satisfactory agreement has been found between the value of the corrosion current calculated from the Stern–Geary equation and the corrosion current found by the extrapolation of the Tafel plot to the corrosion potential in vitro [24a], and to within a factor of three for amalgams in vivo in the heroic experiments of Gettleman et al. [24b].

In our own work [25] an attempt has been made to use modern electrochemical methods to widen the measurement of impedance to a large potential range which encompasses the measured corrosion potential, and produce the high frequency charge transfer resistance–potential, double layer capacity–potential, ohmic resistance–potential and the current–potential curves. Similar measurements have now been made using new electrical equipment, which is optimized for the low currents and high impedances which can be observed in the system. In the present paper some of these new measurements are presented for the dental amalgams Amalcap and Dispersalloy. An interpretation of the results is made in terms of the behaviour of the alloying components in the amalgams.

2. Experimental details

The formal composition of the alloy powders used are Amalcap low copper (Ag 71%, Sn 26%, Cu 3%), Amalcap high copper (Ag, Sn, Cu 20%) and Dispersalloy (Ag 70%, Sn 17%, Cu 11%, Zn 1%), where the quantities are wt %. The Dispersalloy and the high-copper Amalcap amalgams are said to be gamma-2 phase free. The Amalcap is distinguished from the Dispersalloy by the absence of Zn. The Amalcap low-copper sample 35HA was hand packed according to usual dental practice. The hand-packed Amalcap high-copper sample was labelled 36HA. The Dispersalloy sample was labelled 37HD for the hand-packed sample. The speculum metal was a commercial sample, having the composition Cu_3Sn, which approximates electrochemically to the eta2 phase (Cu_6Sn_5) postulated to occur in high copper-containing dental amalgams. A sample of Sn–Hg alloy was prepared by melting the components together and had the com-

position Sn 88.9 at.%, Hg 11.1 at.%. It approximates to the pure gamma-2 phase. The copper was 99.99% pure and the zinc 99.999%. The samples were made up into discs of 12.7 mm diameter which were potted in a suitable non-conducting casting polyester compound (ALPOLIT VUP 9157) to make the electrode. These were held in a suitable holder and the area to be investigated was defined by a neoprene O-ring exposing $0.8\,cm^2$ to the solution. The results obtained were independent of the pressure on the O-ring and similar to results obtained with specimens that were only varnished on the sides. Visual examination after each run showed a uniform coverage with corrosion, and no evidence of crevice corrosion.

Difficulties occurred in making a stable conducting contact to the back of the amalgam discs. Originally a contact was made by pressing a screwed metal spike against the amalgam disc. However over many hours this tended to fail due to creep of the amalgam. This was inferred from the electrochemical measurements which suddenly showed a large change in resistance of about a $M\Omega$. For the samples described here the contact was made by quickly soldering a connecting wire to the unexposed edge of the amalgam disc. During this operation the disc was placed on a cold inert metal heat sink.

The Ringers solution was made up from BDH tablets and triply distilled water. At two-thirds concentration it contains, in gl^{-1}, NaCl 6.0, KCl 0.28, $CaCl_2$ 0.32 and Na_2HCO_3 0.13.

In order to control the potential of the working electrode with respect to a reference electrode and Luggin capillary a potentiostat was developed which is optimized for low-current/high-impedance electrode systems. This was used in conjunction with the previously developed computer system for electrode kinetic measurements.

The computer-aided measurement system [26] was used to undertake the electrochemical measurements. From a menu of experimental measurements steady current–potential and impedance (as a function of frequency)–potential data were accumulated over the potential range -1400 to $-100\,mV$ SCE in 10-mV steps. Data analysis of the impedance was based upon the equation

$$(Z(\omega) - R_\Omega)^{-1} = R_{ct}^{-1} + j\omega C_{dl} \qquad (1)$$

where $Z(\omega)$ is the measured impedance, R_Ω is the ohmic resistance of the electrolyte, R_{ct} is the charge transfer resistance, C_{dl} is the double layer capacity and ω is the angular frequency of the a.c. potential. The high-frequency charge transfer resistance–potential and double layer capacity–potential plots shown in this paper were deduced from this equation and produced as a graphical output.

3. Results

3.1. In vivo corrosion potential measurements

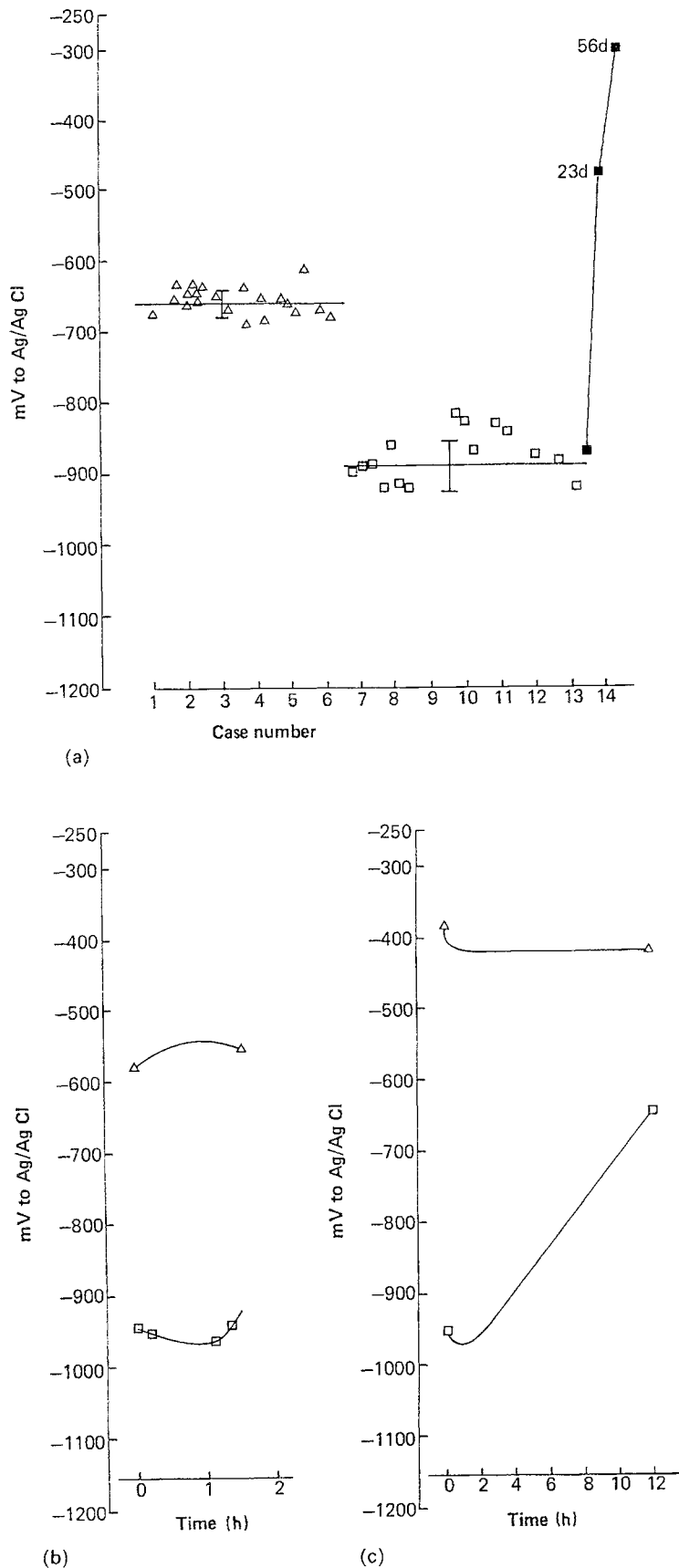Corrosion potential measurements in the mouth of

(a)

(b)

(c)

Fig. 1. Potentials of low-copper and non-zinc amalgam (Amalcap, △) and high copper + zinc amalgam (Dispersalloy, □). (a) Potentials of fresh amalgam apicectomy plugs to Ag/AgCl reference electrode. Horizontal line is the average potential and the error bar is the standard deviation. Case 14, ■, shows the time evolution of the potential of a new Dispersalloy filling over 56 days. (b) Typical potentials for Amalcap, △, and Dispersalloy, □, in a commercial phosphate buffer (pH 6.6, BDH, 4 tablets 100 ml^{-1} water) in natural air. The curves are continuous, only sample points are indicated. (c) Typical potentials for Amalcap, △, and Dispersalloy, □, in two-thirds Ringers solution with natural air. The data represent the average of three curves. The curves are continuous, only sample points are indicated.

amalgams used in apicectomies are shown in Fig. 1. Amalcap and Dispersalloy have been used in these investigations. Apicectomies, in which a small plug of amalgam of about 1 mm^3 is used to seal the root canal at the apex of the tooth root, were used as they are, in principle, free from other influences such as zinc phosphate cement or calcium hydroxide linings. The

corrosion potential measurements were carried out [27] using a voltmeter (Thirlby 1503 HA) having a high input impedance (1000 MΩ) and a specially constructed probe. The probe consisted of a stainless steel wire of 0.8 mm diameter with a tight-fitting PTFE sleeve coming to within 0.3 mm of the tip, which was ground perpendicular to the axis. This was screened to

1.6 mm from the tip by a close-fitting stainless steel tube with an outer insulating rubber sleeve. A mini BNC connector facilitated connection to a coax cable. The exposed tip of the inner wire had a sharp edge which easily made metal-to-metal contact with the amalgam surface. The probe was sterilized by autoclaving at 125° C before each use. Because the exposed tip area was much smaller than the amalgam surfaces, the measured potentials were found to be identical with those from embedded wire.

The reference electrode was a commercial silver-silver chloride electrode. Comparison was made with freshly placed amalgam fillings with similar results. The astonishing fact about these measurements was their reproducibility. Fresh apicectomy plugs of Amalcap had a potential about − 650 mV and Dispersalloy plugs of about − 850 mV. For orientation purposes various redox potentials were calculated from the Nernst equation, assuming a solution activity of 10^{-3} M. The values are in general agreement with the deductions from the kinetics measurements, given below, about the electrode reactions which are occurring at particular potentials. Old apicectomies have a characteristic potential of about − 300 mV which is some hundreds of mV more positive than the fresh samples. This approaches the potentials which are observed for old fillings in the mouth [28].

3.2. In vitro steady current–potential and high frequency impedance–potential measurements

The steady state current–potential curves were determined for each of the samples. At each potential of the steady state current–potential curve high frequency impedance measurements were carried out. The resulting measurements were resolved, using Equation 1, into the high frequency charge transfer resistance–potential and the high frequency double layer capacity–potential curves. A restricted frequency range was used in the measurement of impedance, so no low frequency relaxation processes are included in the measurements. The advantage of measuring the impedance simultaneously with the current is that the charge transfer resistance–potential curve and the capacity–potential can be compared with the current–potential curve. In principle the impedance-derived curves should indicate what part of the current is due to the interfacial electrochemical reaction and give an indication of the state of the surface. Also the charge transfer resistance–potential curve, as it is a derivative, is likely to be a more sensitive indicator of the electrochemical reactions that are occurring than the current. The electrochemical reactions are all of the metal dissolution–passivation type, and of necessity involve varying surface roughness with potential. The roughness of the electrodes caused some problems as this introduced an extra frequency dependence into the current response during impedance measurements. In the present work this was a second order effect and the effect was reduced in importance by weighting the low frequency results more highly than the high fre-
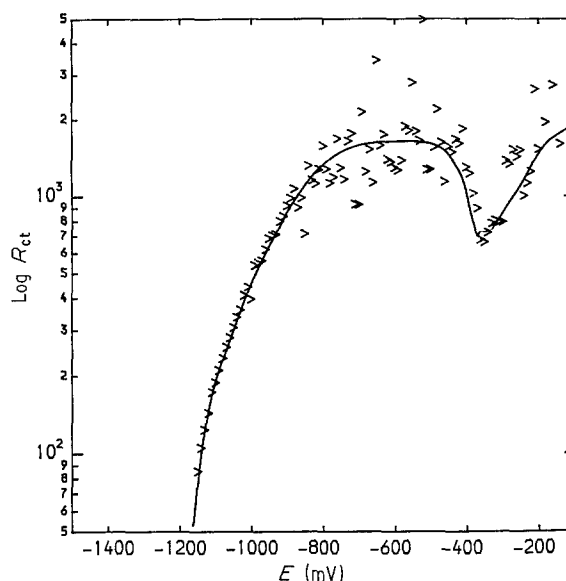

Fig. 2. Steady state behaviour for Speculum metal (Cu–Sn) in two-thirds Ringers solution in the absence of oxygen. The freshly polished electrode was investigated by changing the potential stepwise in 10-mV steps, in the positive direction. Log (charge transfer resistance)–potential curve.

quency. This procedure gave the best fit of Equation 1 to the experimental data.

Speculum metal which contains tin and copper has a charge transfer–potential curve, Fig. 2, which has one minimum at about − 350 mV.

It is interesting that the curve for a pure copper electrode in two-thirds Ringers solution, over the potential range $E = -1400$ to − 100 mV, has no minima. The results show a lowering of the charge transfer resistance at the extremes of potential. At about $E = -1000$ mV the hydrogen evolution reaction starts to become significant, and at about $E = -400$ mV active copper dissolution occurs. In this particular solution, over the potential range − 1400 to − 100 mV there is no sign of a passivation reaction.

Figure 3 shows the charge transfer–potential curve for an alloy containing only tin and mercury. It appears that the hydrogen evolution reaction starts at about $E = -1200$ mV. There are three features which can be attributed to Sn, a minimum at about − 850 mV, an incipient minimum at about − 550 mV and the start of a large diminution of charge transfer resistance at about $E = -400$ mV.

The corresponding curves for Amalcap in Fig. 4a (low copper) and in Fig. 5a (high copper) have essentially the features of speculum metal, with some significant differences. The low copper (35HA)-containing Amalcap charge transfer resistance–potential curve has minima at − 850, − 500 and a large minimum at − 300 mV. It is tempting to attribute these three minima to the Sn to Sn(II), the Sn to Sn(IV) reaction and finally the dissolution and passivation of, say, a tin–copper alloy. It is interesting that Cu itself at potentials up to − 100 mV does not have similar features. The current–potential curve, Fig. 4b, has complementary features to the charge transfer–
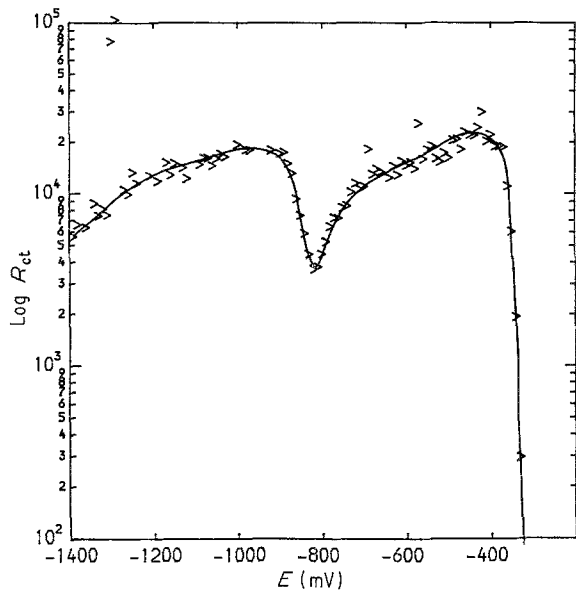
Fig. 3. Steady state behaviour for Sn-Hg alloy in two-thirds Ringers solution in the absence of oxygen. The freshly polished electrode was investigated by changing the potential step-wise in 10-mV steps, in the positive direction. Log (charge transfer resistance)-potential curve.

metals. The films that are formed can also be readily reduced.

The high Cu Amalcap, Fig. 5a, showed similar minima to the low-copper samples, however the minima have higher values of the charge transfer resistance, especially at the potentials of the Sn-Cu alloy dissolution, at -300 mV. The current-potential curve, Fig. 5b, also shows lower currents at the positive potentials. The capacity-potential curve, Fig. 5c, shows significant differences from the low-Cu amalgam, mainly when the films are reduced. A very much larger peak is observed for the low copper-containing amalgam (not shown).

The Dispersalloy samples in two-thirds Ringers solution in the absence of dissolved oxygen, Fig. 6a, showed very similar characteristics to the high-Cu Amalcap, but with an obvious difference. There is a large additional minimum due to the zinc dissolution reactions at around -1100 mV. This has been confirmed by measurements on pure zinc in two-thirds Ringers solution. For pure zinc starting at -1500 mV a minimum was not observed in charge transfer resistance up to a potential of -950 mV, which suggests that in the experimental potential range zinc does not passivate. The minimum, at about -1125 mV in the Dispersalloy experiments, Fig. 6a, may be due mainly to zinc depletion effects. In each case the corresponding double layer capacity-potential curve has been obtained. A typical example is shown in Fig. 5c. The curves, which have some distinguishing features, how-

potential curve, and an active-passive transition at about -250 mV. It is clear that the electrode surface is quite active. The current and the charge transfer resistance show that the various passivation reactions, on the time scale of these measurements, are not very effective at preventing the dissolution of the
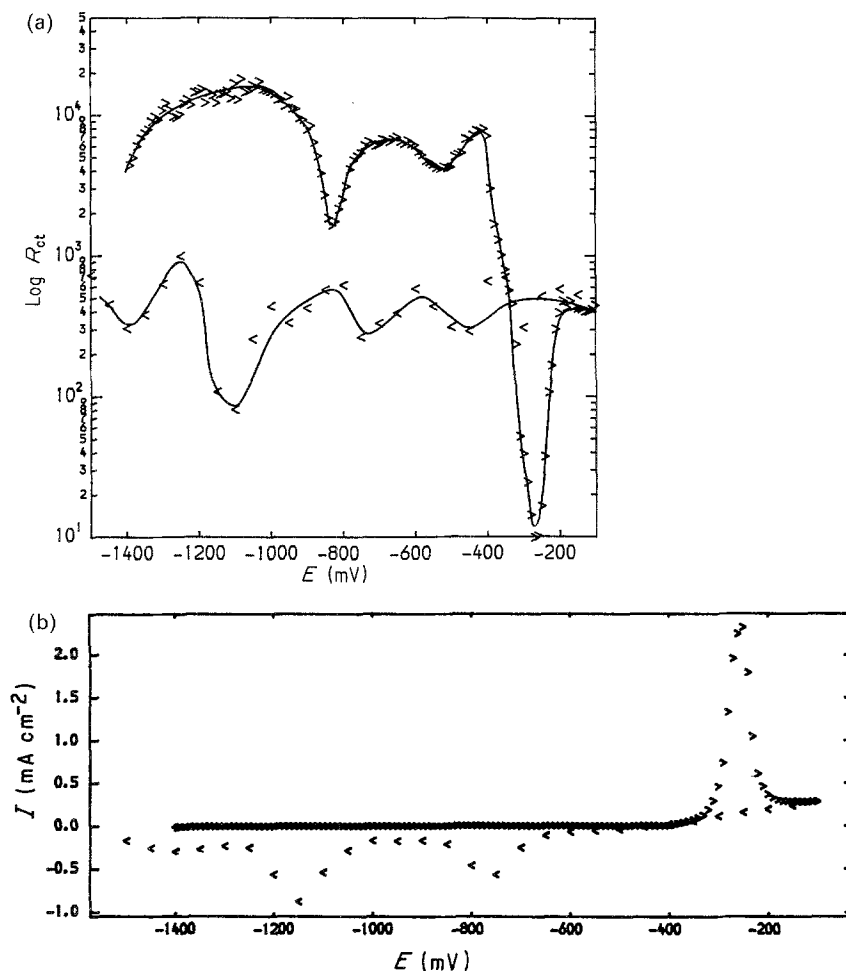

Fig. 4. Steady state behaviour for Amalcap (sample 35 HA, low copper) in two-thirds Ringers solution in the absence of oxygen. The freshly polished electrode was investigated by changing the potential step-wise in the positive direction, and then in the negative direction. (a) Log (charge transfer resistance)-potential curve. (b) Current-potential curve.
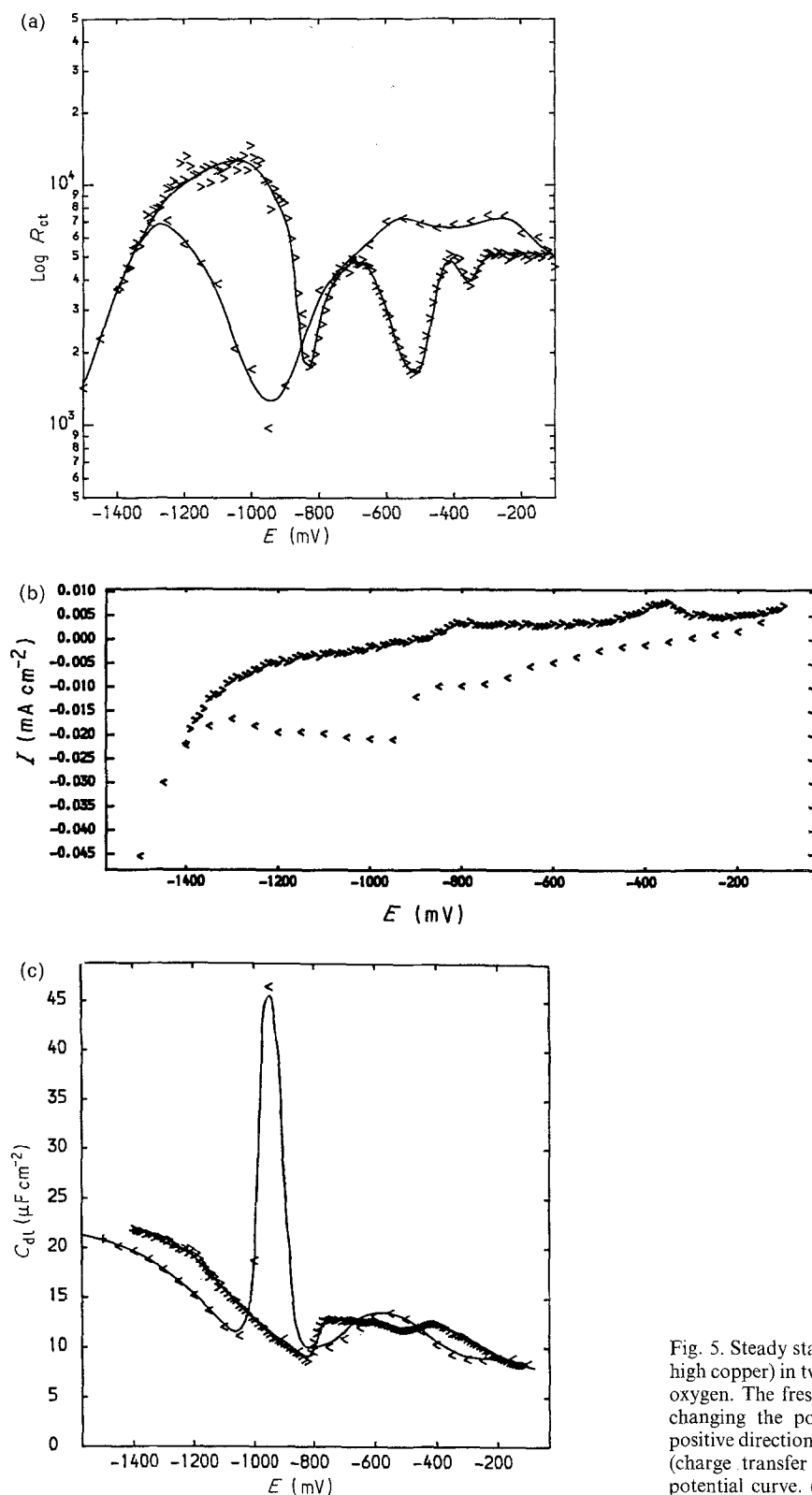
Fig. 5. Steady state behaviour for Amalcap (sample 36 HA, high copper) in two-thirds Ringers solution in the absence of oxygen. The freshly polished electrode was investigated by changing the potential step-wise in 10-mV steps, in the positive direction, and then in the negative direction. (a) Log (charge transfer resistance)-potential curve. (b) Current-potential curve. (c) Double layer capacity-potential curve.

ever are fairly similar. This reflects the fact that the amalgams are mainly mercury and silver which at the potentials investigated are inert. However, in this example, the capacity does increase at about $-850\,mV$ suggesting that the surface roughens as the tin dissolves. There is also a large peak on the return potential sweep as the copper-containing layer is reduced.

3.3. Analysis for solution tin ions by polarography

This work was carried out to assess the solubility of the possible solution soluble ions and to compare the expected currents with the experimentally observed ones. Calibration experiments for zinc ions in 1 M HCl and two-thirds Ringers solution showed a satisfactory concentration dependence of the polarographic wave and a half-wave potential of $-1600\,mV$ vs silver–silver chloride.

Experiments with $SnCl_2$ solutions in 1 M HCl gave a half-wave potential of $-590\,mV$ and for $SnCl_4$ solutions in 1 M HCl gave a half-wave potential of $-520\,mV$.
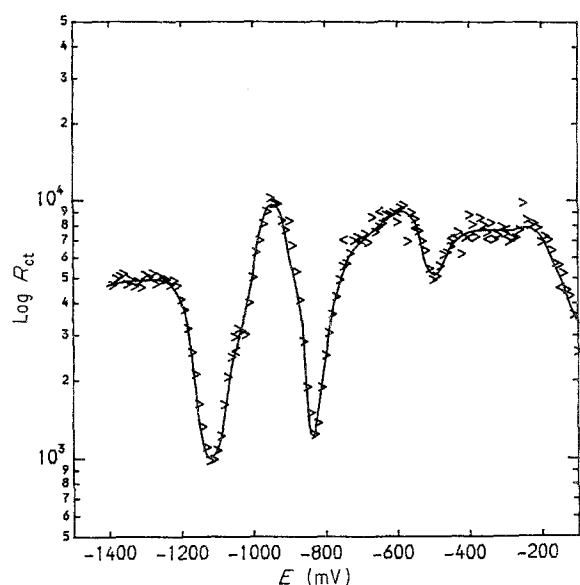
Fig. 6. Steady state behaviour for Dispersalloy (sample 37 HD, high copper) in two-thirds Ringers solution in the absence of oxygen. The freshly polished electrode was investigated by changing the potential step-wise in 10-mV steps, in the positive direction, and then in the negative direction. Log (charge transfer resistance)–potential curve.

Polarography was used to investigate the solubility of $SnCl_2$ and $SnCl_4$ in two-thirds Ringers solution. Below 10^{-3} M solutions $SnCl_2$ showed the correct dependence of the limiting current on concentration and a half-wave potential of -540 mV. Below about 10^{-4} M $SnCl_4$ solutions showed little precipitation and a half-wave potential of -520 mV. In both cases it was necessary to improve the wave by adding 1 ml of concentrated HCl to the cell (of 10 or 20 ml capacity) before analysis.

It is useful to convert these solubilities into currents for the free dissolution of ions, for comparison with the observed corrosion currents, and the oxygen limiting current. For Sn^{2+} the diffusion current is some $200 \mu A\,cm^{-2}$ (the diffusion coefficient $D = 10^{-5} cm^2 s^{-1}$, the diffusion distance $\delta = 10^{-2} cm$). The value for Sn^{4+} is about $40 \mu A\,cm^{-2}$. These figures represent maximum currents that are feasible.

3.4. *Analysis for solution ions by atomic absorption spectroscopy*

Analysis can be readily carried out for silver and mercury ions in solution. In two-thirds Ringers solution silver ions had a measured solubility of $0.32 \mu g$ ml^{-1} and mercurous ions of $33 \mu g\,ml^{-1}$. In a similar way to the dissolution of tin these solubilities could be translated into currents of $0.6 \mu A\,cm^{-2}$ for silver dissolution and $32 \mu A\,cm^{-2}$ for mercury dissolution. Neutral mercury is thought to have a solubility of $0.3 \mu mol\,l^{-1}$ in distilled water at $25°C$ [29].

4. Discussion

The results of the electrochemical investigations can be compared with the theoretical results for a redox reaction. The characteristic behaviour of a redox reaction, which automatically includes the metal deposition–dissolution type of reaction, represents the basic electrode kinetic model against which all electrochemical reactions can be tested. In general, for the reaction

$$A + e \underset{k_b}{\overset{k_f}{\rightleftharpoons}} B \qquad (2)$$
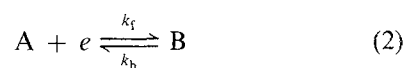
where A and B are redox components and k_f and k_b are the electrochemical rate constants. If these rate constants are defined by

$$k_f = k^0 \exp\{-2.303\,(E - E^0)\,b_c^{-1}\} \qquad (3)$$

$$k_b = k^0 \exp\{2.303\,(E - E^0)\,b_a^{-1}\} \qquad (4)$$

where b_c and b_a are characteristic Tafel slopes, then the current–potential curve is represented by the equation

$$i = F(k_b C_B^s - k_f C_A^s) \qquad (5)$$

where F is the Faraday, and C_A^s and C_B^s are the surface concentrations. The high-frequency charge transfer resistance $(\sqrt{(D/\omega)} \ll \delta)$ is given by

$$R_{ct}^{-1} = F\left(C_B^s \frac{dk_b}{dE} - C_A^s \frac{dk_f}{dE}\right) \qquad (6)$$

The surface concentrations are determined by the steady state fluxes of A and B in a Nernst diffusion layer. Equations 5 and 6 define the connection between the current and the charge transfer resistance. If the diffusion coefficients of A and B and the rate constants k_f and k_b are known, then the surface concentrations can be determined. The method that has been developed in this laboratory is to express the solutions for the surface concentrations in matrix form and calculate the impedance from current–potential data and vice versa.

On the other hand in electrochemical systems and under conditions where diffusion is dominant another resistance can be measured, which is the gradient of the steady state current–potential curve. Its value can be found by inserting the surface concentrations in Equation 5 and differentiating with respect to potential. In the limit when the electrochemical rates k_f and k_b are small compared to DA/δ and DB/δ then both resistances become equal to

$$R_{ct}^{-1} = F\left(C_B^b \frac{dk_b}{dE} - C_A^b \frac{dk_f}{dE}\right) \qquad (7)$$

where C_A^b and C_B^b are bulk concentrations and the charge transfer resistance and current have a simple form which can be tested with the experimental data. When the electrode surface is partly covered by a film the standard rate constant and the diffusion coefficient can both be reduced, and a similar theory is also expected to apply, although with different parameters. Although the above theory, with appropriate extensions, can be used as a convenient model for the dissolution of a single phase (the corrosion of iron is a much-investigated example [30]) the principles

which should be used for alloy dissolution are less certain; see below for a discussion of the correlation of theory and experiment for the dental amalgams. Two recent papers [31, 32] have investigated the dissolution of binary alloys. The steady state dissolution reaction can involve simultaneous or selective dissolution of the two components.

The electrochemistry of the dissolution of the pure metal components in simple aqueous electrolytes are reasonably well known. Zinc has a 40 mV Tafel slope and Zn^+ is not expected as an intermediate [33]. It also shows a curved Tafel slope under some conditions, also observed in this investigation, which is said to be due to the dissolution of the metal at a limited number of active sites [34, 35]. Copper dissolution has a 40 mV Tafel slope and Cu^+ is an observed intermediate. Copper forms an oxide under some conditions [36]. Tin dissolution has 2-electron active–passive regions, probably due to Sn(II) and Sn(IV) [37]. In phosphate-containing electrolytes the films can also contain phosphate [37, 38]. The charge transfer resistance values for all the amalgams are, over most of the potential range, similar to the low-frequency resistance. All the Amalcap samples have three minima. A distinction between the curves is noticeable at the most positive minimum which depends strongly on the copper content. Speculum metal which contains only copper and tin has a single minimum. Dispersalloy, which is a high copper-containing alloy, also contains zinc and this is evident in the curves which all have four minima. The mercury–tin alloy curve has two minima at − 850 and − 550 mV which are common to the Amalcap and Dispersalloy samples. The large feature at − 400 mV must be attributed to a transpassive dissolution in which the passivating Sn(IV)-containing passive film breaks down and a large amount of tin leaves the sample. In Amalcap and Dispersalloy there are two ways of explaining the minimum at the most positive potentials; either copper stabilizes the Sn(IV)-containing passive film so that it does not break down as in the tin–mercury alloy, or a new phase containing copper and tin is oxidized. A further factor is that on ageing for a long time (about 6 months) a Dispersalloy sample seems to lose the minimum at − 300 mV and, at these potentials, to behave like a pure copper sample. This behaviour must be looked at in the context of the phases which exist in amalgams. The gamma-2 phase, Sn_8Hg is thought to be the most corrodable. In the so-called non-gamma-2 amalgams this phase is much reduced by the higher copper content of the alloy powder which competes with mercury for tin to gradually form the phases Cu_6Sn_5 or Cu_3Sn. Since phase changes in set amalgam occur by diffusion in the solid this process may continue for many weeks [39, 40]. This is confirmed in the present work by the large dissolution of the alloy containing only the components tin and mercury in amounts close to the composition of the gamma-2 phase. As shown in the Figs 2–5a, as copper is added this dissolution is substantially reduced.

4.1. Corrosion rate from electrochemical measurements

Under the conditions of Equation 6, the corrosion current (in the absence of oxygen) is related to the charge transfer resistance at the corrosion potential (in the absence of oxygen) by

$$b_a = 2.303 i R_{ct} \qquad (8)$$

Equation 8 is a basic relation which should determine, to a first order of approximation, the interconnection between current and charge transfer resistance data. In order to test this equation the quantity b was calculated at all potentials for the data of Fig. 6, and also for pure zinc. The charge transfer resistance–potential and the current–potential curves have complementary features and, as observed, should correlate strongly together. The features in the charge transfer data are, however, separated more clearly from one another than in the current–potential data. The indications are that for the dissolution of zinc and tin to tin(II), which must be the simplest as they occur on the initially bare surface, the values of b seem to be consistent with a reversible reaction. This is explained by the fact that the measurements are made with stationary electrodes and hence with a large diffusion layer, and then with an oxide-containing film of increasing thickness. The simplest model for this situation is given by inserting in the above equations for i and R_{ct} the concentration for the species A given by the Nernst equation, i.e. the electrochemical case of a.c. on reversible d.c. This assumption is consistent with the standard potential values given in the literature. The zinc dissolution in the plot of b against potential is not well separated from the hydrogen evolution reaction. In the charge transfer–potential plot of Fig. 6, most of the dissolving species are clearly differentiated. The characteristic Tafel slopes in the charge transfer resistance–potential plot, for both the zinc and tin to tin(II) reactions, are about 120 mV. Presumably this is evidence for progressive oxide formation, or depletion effects, which are superimposed on the basic a.c. on reversible d.c. pattern, provided the potential is not too positive, say up to − 600 mV in Fig. 6. The electrochemistry of the successive dissolution of alloy components is complicated and is under further investigation. The currents in the absence of oxygen for a 0.79 cm² electrode surface, at the corrosion potentials given in Fig. 1 are, for Dispersalloy (37HD) $i = 1.1 \mu A$ at $E = − 850$ mV, for Amalcap (36HA) $2.6 \mu A$ at $E = − 650$ mV and for Amalcap (35HA) $2.3 \mu A$ at $E = − 650$ mV. The experimental results presented here demonstrate that corrosion at − 850 mV is predominantly tin, and at − 650 mV is also tin; see Figs 3, 4a and 5a. These figures can be compared with wear rate measurements for Dispersalloy which range from 36 [41] and 54 [42] $\mu m \, year^{-1}$ and the figures of Espevik and Mjoer [43] of 2.5–3 years for a depth of corrosion damage to 200 μm under the occlusal surfaces of low-copper amalgam fillings equivalent to 66–80 $\mu m \, year^{-1}$, and the clinical findings of Derand [44] of 235 μm corrosion depth for

the high-copper Dispersalloy amalgam over 4 years equivalent to 59 (SD 13) μm year^{-1}. If one takes a figure for wear of only 25 μm year^{-1} and a density of 11 g cm^{-3} for the dental amalgam and an area of 1 cm^2 this is equivalent to a removal of about 75 μg of amalgam day^{-1}. About half of this by weight will be mercury if the composition is the same as the original material. A typical adult molar or premolar tooth has an occlusal area of about 0.5–1 cm^2 so that a single amalgam filling with an occlusal area of 0.4 cm^2 may, on average, release through wear 15 μg day^{-1}, half of the maximum allowed dose rate of mercury from all sources (of 30 μg day^{-1}), as specified by the US Environmental Protection Agency [47]. It is interesting to calculate the equivalent current by assuming that the divalent tin or univalent copper is the corroding phase. With an atomic weight per unit electronic charge of 59.3 or 63.5, respectively and constituting together about 14.5 and 14.0% by weight, respectively for Amalcap and Dispersalloy amalgams, this amounts to 10.9 and 10.5 μg day^{-1} of tin and copper in the amalgam, and hence average corrosion currents of 0.2 and 0.19 μA, respectively. For 4-valent tin and divalent copper these currents will be doubled. The potential of the amalgams during *in vivo* wear is variable [27] but Marek [45], using aerated artificial saliva and both low- and high-copper amalgams previously uncorroded, has shown that soft fabric or soft leather immersed in artificial saliva and wiped across the amalgam surface at a pressure of 0.5 MPa, only slightly more than that required to maintain contact, removed the surface passivating film and caused an abrupt change in the corrosion potential of about -250 mV for low-copper amalgams and -350 mV for Dispersalloy. This was associated with a large change in corrosion current. Marek concludes that abrasion increases the corrosion rate by destruction of the passivating film and that repassivation is relatively slow. If the amalgams sit at the potentials given in the present paper and in [28] then wear experimental data are consistent with an electrochemical mechanism in which the corrosion films removed by any method are rebuilt by a current flow due to tin and copper ions. The amount of the current should be similar to those of the relatively active surfaces investigated in this paper.

5. Conclusions

The main conclusions can be summarized, as follows.

(1) The charge transfer resistance–potential curves, in absence of dissolved oxygen, clearly show the successive electrochemical dissolution of the metals in the dental amalgams as the potential is increased. By comparing the *in vivo* corrosion potential measurements on the fresh apicectomies with the charge transfer–potential measurements it can be deduced that, initially, the metals zinc and tin (for Dispersalloy) and tin (for Amalcap) are the corroding metals. It can be surmised that as the metal dissolves mercury- and silver-rich phases remain. Only at

positive potentials, well outside the range of the apicectomy measurements, is electrochemical mercury corrosion possible. There is no evidence, at the moment, that apicectomies or dental fillings can ever reach these potentials, except when they are in contact with other metals, such as gold, which should be avoided both for this reason and to prevent galvanic currents.

(2) The electrochemical corrosion rates from the fresh amalgams of the metals zinc, tin and copper are similar to the overall long-time mechanical wear rate which is given in the literature. This suggests a coupling of the mechanical and electrochemical effects. A comparison of the measured corrosion potentials and the charge transfer–potential curves confirms that the amalgams are protected from the direct electrochemical dissolution of mercury by the dissolution of other metals.

(3) In addition to the possible indirect electrochemical mechanism for mercury loss (see above), neutral mercury has a substantial evaporation rate from untarnished amalgams, limited by the solid state diffusion within the amalgam, and perhaps the transition of the gamma-1 phase, Ag_2Hg_3 or more probably $Ag_{22}SnHg_{27}$ to the lower mercury beta-1 phase, AgHg [14], and also, perhaps, the decomposition of a Cu–Hg phase, probably Cu_4Hg_3 [46]. Some quantitative data is available in the literature [8, 9]. Qualitative measurements made in our work tend to confirm the view that the *in vivo* dissolution rate is additional to the electrochemical corrosion wear rate and as the amalgam surface roughens by the stripping off of tin and copper a greater area of the remaining Ag–Hg phases becomes available for dissolution. The gamma-1 phase has been detected after *in vivo* corrosion of Dispersalloy [48–50] and attributed to the leaching of Cu–Sn from gamma-1 grain boundaries.

(4) The mechanism for setting the *in vivo* corrosion potential is not known. The electrochemical *in vitro* evidence presented here suggests that in the early stages it is the hydrogen evolution reaction which sets the potential, and at later times control moves to the oxygen reduction reaction. Under these conditions the corrosion potential moves to more positive values. *In vivo*, there may also be some as yet unknown biological redox systems which may be involved, in preference to the oxygen reduction reaction, in controlling the corrosion potential and hence the metal corrosion rate.

References

[1] J. E. Abraham, C. W. Svare and C. W. Frank, *J. Dent. Res.* 63 (1984) 71.
[2] B. Moeller, *Swed. Dent. J.* 2 (1978) 93.

[3] M. L. Oldstad, R. I. Holland, N. Wandel and A. H. Petter-sen, *J. Dent. Res.* **66** (1987) 1179.

[4] R. R. White and R. L. Brandt, *JADA* **92** (1976) 1204.

[5] M. Jolly, A. J. Moule, R. W. Bryant and S. Freeman, *Br. Dent. J.* **160** (1986) 434.

[6] P. O. Lind, B. Hurlen, T. Lyberg and E. Aas, *Scand. J. Dent. Res.* **94** (1986) 448.

[7] D. Brune and D. M. Evje, *Scand. J. Dent. Res.* **92** (1984) 165.

[8] M. J. Vimy and F. L. Lorscheider, *J. Dent. Res.* **64** (1985) 1069.

[9] M. J. Vimy and F. L. Lorscheider, *J. Dent. Res.* **64** (1985) 1072.

[10] M. J. Vimy, A. J. Luft and F. L. Lorscheider, *J. Dent. Res.* **65** (1986) 1415.

[11] S. Olsson and M. Bergman, *J. Dent. Res.* **66** (1987) 1288.

[12] M. J. Vimy and F. L. Lorscheider, *J. Dent. Res.* **66** (1987) 1289.

[13] J. R. Mackert, *J. Dent. Res.* **66** (1987) 1775.

[14] T. Okabe, *Dent. Mater.* **3** (1987) 1.

[15] R. G. Craig, *Dent. Mater.* **2** (1986) 91.

[16] See Chaps 1 and 2 in 'Biocompatibility of Materials, Vol. 3, Restorative Materials' (edited by D. C. Smith and D. F. Williams), C.R.C. Press, Boca Raton, Florida (1982).

[17] Van Noort *et al.*, *J. Dent.* **15** (1987) 99.

[18] 'Restorative Dental Materials', 7th edn (edited by R. G. Craig), C. V. Mosby, St Louis (1985).

[19] S. J. Marshall, J-H. C. Lin and G. W. Marshall, *J. Biomed. Mater. Res.* **16** (1982) 81.

[20] S. J. Jensen, *Scand. J. Dent. Res.* **90** (1982) 239.

[21] J. H. C. Lin, G. W. Marshall, S. J. Marshall, *J. Biomed. Mater. Res.* **17** (1983) 913.

[22] G. Ravnholt, *Scand. J. Dent. Res.* **94** (1986) 533.

[23] L. E. Moberg, *Scand. J. Dent. Res.* **95** (1987).

[24a] R. Grajower and E. H. Greener, *J. Biomed. Mater. Res.* **14** (1980) 547.

[24b] L. Gettleman, F. Hadley Cocks, L. A. Darmiento, P. A. Levine, S. Wright and D. Nathanson, *J. Dent. Res.* **59** (1980) 689.

[25] M. J. Gross and J. A. Harrison, *J. Appl. Electrochem.* **16** (1986) 265.

[26] J. A. Harrison, 'Comprehensive Chemical Kinetics', Vol. 29 (in press).

[27] M. J. Gross, K. B. Fanibunda, I. D. McGregor and J. A. Harrison, in preparation.

[28] K. Nilner and R. I. Holland, *Scand. J. Dent. Res.* **93** (1985) 357.

[29] W. Gerrard, 'Gas Solubilities', Pergamon Press, Oxford (1980) p. 412, Table 179.

[30] W. J. Lorenz and K. E. Heusler, in 'Corrosion Mechanisms' (edited by Florian Mansfield), Dekker, New York (1987).

[31] S. Rambert and D. Landolt, *Electrochim. Acta* **31** (1986) 1421.

[32] S. Rambert and D. Landolt, *Electrochim. Acta* **31** (1986) 1433.

[33] J. A. Harrison, D. R. Sandbach and P. J. Stronach, *Electrochim. Acta* **24** (1979) 179.

[34] J. A. Harrison and D. R. Sandbach, *J. Electroanal. Chem.* **85** (1977) 125.

[35] E. Schmidt, J. Hitzig, J. Titz, K. Juttner and W. J. Lorenz, *Electrochim. Acta* **31** (1986) 1041.

[36] M. M. Lohrengel, J. W. Schultze, H. D. Speckmann and H-H. Streblow, *Electrochim. Acta* **32** (1987) 733.

[37] H. Do Duc and P. Tissot, *J. Electroanal. Chem.* **102** (1979) 59.

[38] B. N. Stirrup and N. A. Hampson, *J. Electroanal. Chem.* **73** (1976) 189.

[39] S. J. Marshall and G. M. Marshall, *J. Biomed. Mater. Res.* **13** (1979) 395.

[40] N. Sarkar, *J. Oral. Rehab.* **6** (1979) 1.

[41] F. H. J. Hendriks, H. Letzel and M. M. A. Vrijhoef, *J. Dent. Res.* **656** (1986) IADR abstract No. 903.

[42] M. Braem, P. Lambrechts, L. Haspeslagh and G. Vanhele, *Dent. Mater.* **2** (1986) 106.

[43] S. Espevik and I. A. Mjoer, 'Corrosion and Degradation of Implant Materials' (edited by B. C. Syrett and A. Acharya), Am. Soc. for Testing Mat. (1979) STP 684, Philadelphia 316.

[44] T. Derand, *Scand. J. Dent. Res.* **94** (1986) 253.

[45] M. Marek, *J. Dent. Res.* **63** (1984) 1010.

[46] R. W. Bryant, *J. Oral Rehab.* **12** (1985) 37.

[47] T. W. Clarkson, J. Cramner, D. J. Sivulka and R. Smith, Mercury Health Effects Update, Health Issue Assessment Final Report U.S. Environmental Protection Agency, EA 600/8-84-019F (1984).

[48] D. McTigue, C. Brice, C. R. Nanda and N. K. Sarkar, *J. Oral. Rehab.* **11** (1984) 351.

[49] D. B. Boyer, *Dent. Mater.* **4** (1988) 89.

[50] D. Brune, *Int. Endodontic J.* **21** (1988) 135.